RJC

RASĀYAN *J. Chem.*
Vol. 11 | No. 4 |1663 - 1673| October - December | 2018
ISSN: 0974-1496 | e-ISSN: 0976-0083 | CODEN: RJCABP
http://www.rasayanjournal.com
http://www.rasayanjournal.co.in

STUDIES ON THE ADSORPTION OF RHODAMINE-B USING NOVEL NANO CARBON BALLS

V.Priya[1], S.K. Krishna[1,*], V. Sivakumar[2] and P. Sivakumar[3]
[1]Department of Chemistry, Chikkaiah Naicker College, Erode-638004 (TN) India
[2]Department of Chemistry, Sri Vasavi College, Erode-638316 (TN) India
[3]Department of Chemistry, Arignar Anna Govt Arts College, Namakkal-637 002 (TN) India
*E-mail: ragul2022@gmail.com

ABSTRACT
The study demonstrates the facile synthesis of nano-sizedfullerene-like carbon balls named as nano carbon spheres (NCS) and its application for the effective adsorption of a textile dye Rhodamine-B (Rh-B) from the stimulated solution at laboratory scale. The essential controlling factors like pH of the effluent, initial Rh-B concentration and the solution temperature are investigated. The kinetics follows multi-order and Freundlich type of isotherm. The sorption energy-related parameters like ΔG, ΔH and ΔS were also evaluated. The outcome signposts that NCS is a potential material for the sorption of Rh-B with good efficiency.
Keywords: Nanocarbon, Kinetics, Isotherm, Adsorption, Dye, Effluent.

INTRODUCTION

There is a growing concern about the quality of the environment all around the world due to the discharge of various categories of pollutants. The water pollution, in particular, makes a great impact on the healthy human life. Among the pollutants which are added in the water bodies, wastewater containing dyes are a major threat to living things[1]. The presence of an even small amount of a dye prevents the effective penetration of light and retards the primary food production through photosynthesis. Another problem associated with the presence of coloring matter in an aquatic system is the reduced solubility of oxygen, which hinders the evolution of aquatic biota[2].

The dye bearing wastewater creates a lot of adverse effects like allergy, dermatitis, skin irritation and cancer[3]. The intake of dye molecules inside the animal and plant cells creates a lot of mutagenic and teratogenic effects[4]. Many industries like food processing, textile, leather processing, plastic, paper and cosmetic industries are the major uses of various category of large complex organic dye molecules[5-12]. It was estimated that more than 1,00,000 type of dyes are manufactured per annum with an amount of nearly $7x10^5$ metric tons[3]. Out of the above production, every year nearly 100 tons are discharged through wastewaters[13]. The reason for this huge loss of dyes through wastewater is due to their high solubility and high resistance against the convention treatment technologies[14]. Currently, there are many technologies like adsorption, ozonation, photocatalysis,chemical flocculation followed by coagulation, oxidation using air, oxidation with chemicals,flocculation driven by an electric potential, filtration with semipermeable membranes, degradation using electrode potential and microbial degradation are available for the removal of dyes present in the wastewater[15-22]. These methods have some disadvantages like poor efficiency or huge treatment expenses.

Adsorptive removal of dyes using high surface material has a lot of advantages like good efficiency, wide selectivity and simple technology. But the cost of commercial activated charcoal is not affordable to the small-scale industries in developing countries like India. The preparation of an adsorbent in the nano size can give more surface area and thereby removing more amounts of pollutants per unit weight of the adsorbent.The usage of nanocarbon constituents for adsorption of pollutants is most suitable due to the

http://dx.doi.org/10.31788/RJC.2018.1145027

excellent surface to bulk ration. The objective of the research is to prepare a novel nano carbon and analyzing its ability for the adsorption of Rhodamine-B.

EXPERIMENTAL

Materials

All chemicals were used are of analytical grade, purchased and used as received without additional purification. All solutions prepared using double distilled water. Waste engine oil was used for the preparation of carbon ball.

Preparation of Green Catalyst and NCS

The multi-metal catalyst was synthesized in a green procedure using the following steps. The stems of *Alternantherasessilis* was air dried and cut with a mean size of 2 to 5 cm length. It is burnt in a muffle furnace at 750°C for 1 h under a constant flow of Nitrogen at 0.1 bar. The carbon washed with pure water two times followed by alcohol wash, the washed carbon dried in air oven at 110°C for 24 h[23].The carbonized stems of *Alternantherasessilis* were soaked with waste engine oil for about 30 min and then air dried for about 1 h. The air-dried, oil-soaked carbonized stems were kept on a stainless steel grill and it is burnt from the bottom using LPG as fuel mixed with air. The soaked stems will start to burn at its ignition temperature, then the fuel gas (LPG) was cut off and the air inlet is regulated in such a way that, the combustion temperature was controlled at 420 to 470°C. The soot formed during the combustion was collected using a dome-shaped surface of Stainless steel lid (316SS) which is kept over the combustion chamber. The excess exhaust gas allowed to escape through exhaust holes. The ash formed during the combustion process was frequently removed through the discharge opening provided at the bottom of the reactor. The carbon deposited at the inner surface of the stainless steel dome was carefully collected, washed with plenty of distilled water followed by a single alcohol wash. The NCS is activated using a microwave oven at 600w of power at a dwell time of 10 min. The SEM images of NCS were viewed using a Zeiss Electron microscope at a maximum magnification of 41.14 x 10^3 zooming.

Batch Adsorption Studies

Rhodamine-B (Rh-B)a basic dye with a molecular weight of 479.02, formula $C_{28}H_{31}ClN_2O_3$, C.I No. 45170 and the absorption maxima at 543 nm, (E. Merck, India) is used as a model solute for the adsorption studies. A stock solution of 1000 mg/L is prepared using an appropriate amount of dye dissolved in distilled water and further diluted solutions prepared from this stock solution. For the batch mode adsorption studies, 100 mL of dye solution of specified concentration is equilibrated with 100 mg of NCS in 250 mL tight lid reagent bottle (Borosil-R glass bottles) using REMI make an orbital shaker. For the effect of pH, 1M HCl and 1M NaOH solutions are used for the alteration of pH of the solution. After the specified time of agitation, the contents of the flask are centrifuged using Universal make centrifuge at 5000 rpm and the final concentration of the dye solution is estimated by measuring the optical density at the λmax of Rh-B solution (543 nm) using UV-VIS spectrometer (Model : Elico-BL198). All the adsorption experiments have been done in duplicated and the maximum deviations from the two runs are 4% only.

The percentage and amount of dye removed through adsorption are calculated using the following relationships.

$$\text{Percentage of dye removed} = \frac{Initial\ concentration(C_0) - Concentration\ at\ time\ t\ (C_t)}{Initial\ concentration\ (C_0)} x100 \quad (1)$$

The quantity of Rh-B removed per unit quantity of NCS (q_t)

$$= (C_0 - C_t)\frac{V}{W} \ \text{mg/g} \quad (2)$$

Where, V is the volume of dye solution in mL and W is the weight of adsorbent in grams.

Kinetic and Isotherm Models used[3,24]

The four different kinetic models such as the pseudo-first-order model, pseudo-second-order model, Elovich model and Intra-particle diffusion model were used to assess the mechanism of dye adsorption.

Langmuir and Freundlich isotherm models were used for equilibrium temperature studies. Energy changes of the sorption processes were evaluated with the help ofVan't Hoff plot.

Table-1

Model	Equation
Pseudo-first order model	$\log(q_e - q_t) = \log q_e - \frac{k_1}{2.303}t$
Pseudo-second order model	$\frac{t}{q_t} = \frac{1}{k_2 q_e^{\,2}} + \frac{1}{q_e}t$
Elovich model	$q_t = \frac{1}{\beta}\ln(\alpha\beta) + \frac{1}{\beta}\ln(t + t_0)$
Intra-particle diffusion model	$q_t = k_d \,.\, t^{1/2}$
Langmuir model	$\frac{C_e}{q_e} = \frac{1}{Q_0 . b_L} + \frac{C_e}{Q_0}$
Freundlich model	$\log\ q_e = \log\ k_f + \frac{1}{n}\log\ C_e$
Thermodynamic parameters	$\Delta G = -RT ln b_L$ $\Delta G = \Delta H - T\Delta S$ $lnK_C = -\frac{\Delta H}{RT} + \frac{\Delta S}{R}$

RESULTS AND DISCUSSION

General Characteristics

The scanning electron microscopic images of NCS are shown in Fig.-1. As observed from the SEM images of the pure carbon samples, the clusters of carbon nanospheres of sizes ranging between 50 and 80 nm are present. The other characteristics of NCS are given in Table-1(a). The NCS has a pH and pH_{ZPC} blow 7.0, could have been due to the presence of acidic functionalities. As the carbon is nano-sized, the bulk density is very small and the surface area is 700.7 m^2/g, which is comparable with that of commercial variants.

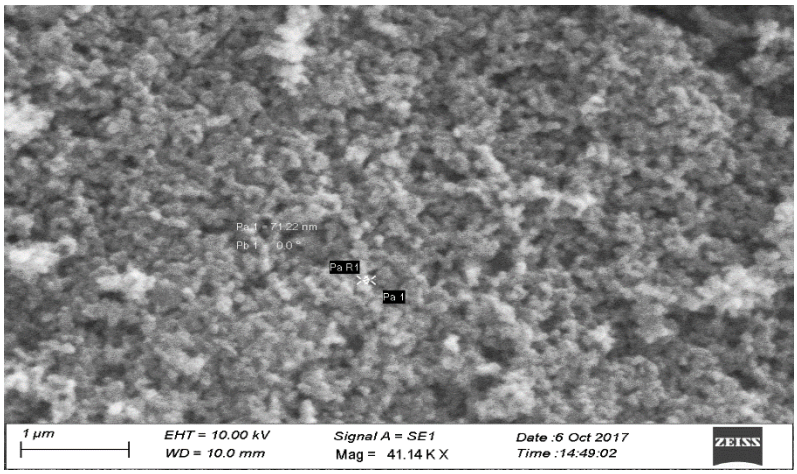

Fig.-1: SEM image of pure NCS

Effect of pH on the Adsorption of Rh-B

One of the most important environmental variables that might be considered for the design and development of a good adsorption system is the solution pH. Most of the dyes in its aqueous solution will exist as an ion. These ionized dye molecule show variable adsorption on varying the solution pH may have a different role.

Table-1: Certain Properties of NCS

S. No.	Property	NCS
1.	pH	6.6
2.	pH_{ZPC}	6.8
3.	Bulk Density, g/mL	0.145
4.	BET Surface Area, m^2/g	700.7
5.	Moisture content, %	11.45
6.	Volatile matter, %	6.62

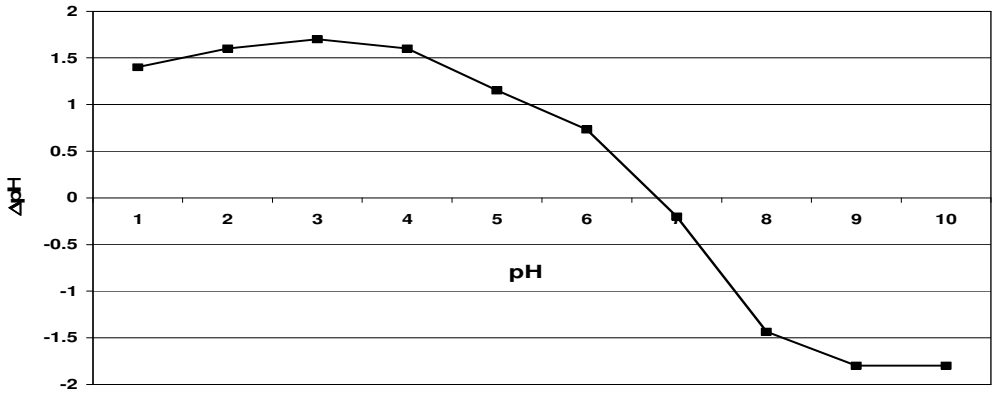

Fig.-2: Plot for the Determination of pH_{ZPC} of NCS

The pH_{zpc} value obtained for the NCS is 6.8, (as shown in Fig.-2). Below the pH of 6.8, the NCS acquires a positive charge and above 6.8, the surface of NCS acquires a negative charge[25,26]. The selected dye Rhodamine-B is a cationic dye, which exists as $Rh\text{-}B^+$ and Cl^- in its aqueous solution. When the solution pH is less than the pH_{zpc} of NCS, the surface of NCSacquires a positive charge and it will repel the positively charged $Rh\text{-}B^+$ ion. As observed from the Fig.-3, the adsorption of Rh-B increases from 49.6% to 82.4% on increasing the solution pH from 2.0 to 7.0.

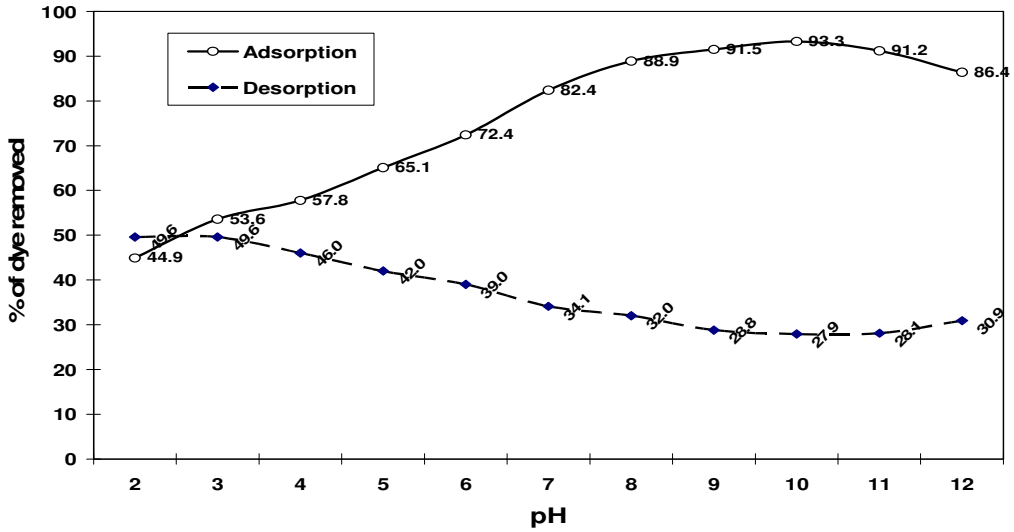

Fig.-3: Effect of pH on the Adsorption of Rh-B Dye

At lower pH, the surface of NCS has great positive and hence repels the dye cations. On increasing the solution pH, the positive charge of NCS surface decreases, which favors the adsorption. When the pH exceeds the pH_{zpc} of NCS, the surface of NCS is negative and further favors the adsorption of $Rh\text{-}B^+$ ions[27]. The maximum Rh-B sorption was achieved at pH of 10.0 and it decreases to 86.4% when the solution pH reaches 12.0.For large scale operations of Rh-B adsorption by NCS, the solution must be adjusted to basic nature (i.e pH of 10.0).

The desorption studies were performed to check the reusability of the novel adsorbent using a known quantity of dye-loadedNCS. As observed inFig.-3, the desorption was maximum at a pH of 2.0 (44.9%) and it decreases on increasing the pH from 2.0 to 12.0. At lower pH, the competitive H^+ will easily displace the Rh-B^+, whereas at higher pH, the OH^-ions will not favor the desorption. The adsorbent can be successfully employed up to 8 cycles with the good quantum of adsorption.

Effect of Initial Rh-B Concentration

The impact of initial Rh-B concentration on its adsorption performance with NCS was evaluated by changing the initial Rh-B concentration from 20 to 100 mg/L for a fixed volume of 100ml and an adsorbent dosage of 100mg. As observed from the fig. 4a, it was clear that the rate of adsorption increases with time and reaches equilibrium at 90 min. In the beginning, the rate of adsorption was rapid, as the bare NCS surface favors the adsorption of Rh-B at a faster rate. Also, the high concentration gradient between the solid-liquid interfaces creates more driving force, which leads high initial adsorption rate. The increase of Rh-B concentration does not have much influence on the attainment of equilibrium. During the progression, the concentration gradient across the solid-liquid interface diminishes and the speed of adsorption also decreases.

When the initial Rh-B concentration increased from 20 to 100 mg/L, the quantity of Rh-B removed by adsorption increases from 19.68 to 79.13 mg/g. Whereas, the percentage of removal of Rh-B decreased from 98.39 to 79.13 % on increasing the initial Rh-B concentration from 20 to 100 mg/L. At lower concentrations, the probability of the availability of surface sites for a given dye molecule is more than at higher concentration. At higher initial concentrations, the number of sorbent sites per given number of the dye molecule is less, which results in lower adsorption percentage[28].

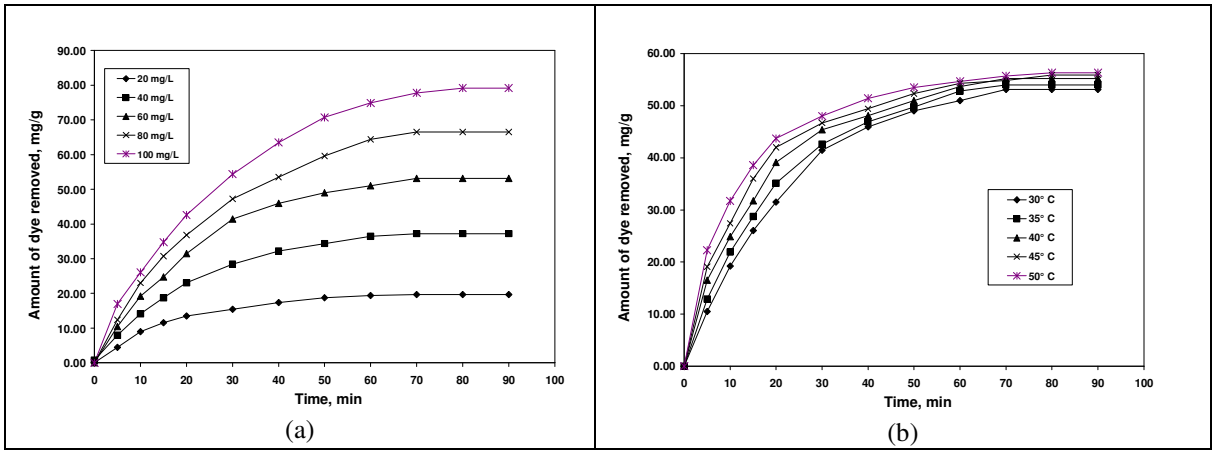

Fig.-4: Variation of Rh-B Adsorption onto NCS (a) Concentration Variation, (b) Temperature Variation

Influence of Temperature

It is a well-known fact that the adsorption of a solute from its solution increases with temperature if it is chemisorption. In the case of physisorption, the rate of adsorption decreases with the increase in temperature. The porous activated materials may have surface functionalities (which favor the chemisorption type of adsorption) and mesopores and micropores (which favors the physisorption type of adsorption). In most of the adsorbent –adsorbate systems, both physisorption and chemisorption may operate simultaneously. In this case, the adsorption of Rh-B on to NCS increasing from 53.14 to 56.33 mg/g for the rise of temperature from 30 to 50°C for a fixed initial dye concentration of 60mg/L as shown in Fig.-4b. The endothermic nature is supported by adsorption increase by raise in temperature[29]. The endothermic nature of the Rh-B adsorption onto NCS will further be confirmed by thermodynamical studies using Van't Hoff plots in the subsequent studies.

Kinetic Analysis

For the design and development of a good adsorption system, it is essential to evaluate the kinetic parameters. This kinetic analysis provides essential details about the adsorption process and its

mechanism[29]. In this study, the already existing kinetic models were used. The mechanism of adsorption was evaluated using the intra-particle diffusion kinetic model.

Pseudo-First Order Kinetic Model

The pseudo-first order plot for the adsorption of Rh-B onto NCS at various initial Rh-B concentration and temperatures are shown in Fig.-5. The results derived from the pseudo-first order rate constant k_1 decreases from 6.425×10^{-2} to 5.366×10^{-2} min^{-1} on increasing the initial Rh-B concentration from 20 to 100 mg/L and it varies from 5.527 to 5.965 x $10^{-2} min^{-1}$ under the range of temperature studied. The q_e calculated from the pseudo-first-order rate equation show similarities with respect to the experimental values under the various concentrations, but not show any sequential variation with that of experimental values under different temperature range. These results (Table-2) indicated that the pseudo-first-order kinetic model describes the adsorption at lower concentrations and temperatures and it deviates at higher concentrations and temperatures.

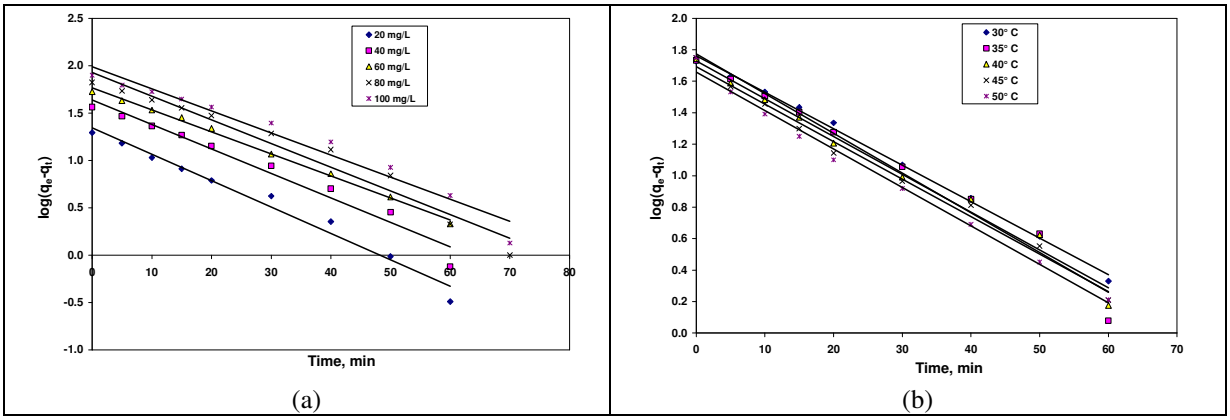

(a) (b)

Fig.-5: Pseudo-First Order plot of Rh-B Adsorption onto NCS, (a) Concentration variation, (b) temperature variation

Pseudo-Second Order Kinetic Model

According to this modal, the adsorption rate of Rh-B on to NCS depends upon any two terms. The pseudo-second-order plot for the adsorption of Rh-B onto NCS at different concentrations and temperature are shown in Fig.-6. The results derived from the pseudo-second-order model are presented in Table-2.

The pseudo-second-order rate constant $k_2$decreases from 2.44×10^{-3} to 0.37×10^{-3} (g/mg/min) on increasing the concentration of Rh-B from 20 to 100 mg/L. But it's value increases when the adsorption system temperature increased from 30 to50° C. The $qe_{(cal)}$ calculated from the pseudo-second-order model show consistent variation with that of experimental $qe_{(exp)}$ under various initial Rh-B concentrations and temperature.

On analyzing the results of the above kinetic models, the first order model is suitable at the beginning of adsorption and in the later stages, the adsorption follows pseudo-second-order kinetics.

Elovich Kinetic Model

The Elovich model is derived based on the assumption of chemisorption type of adsorption of Rh-Bon to NCS (Fig.- not shown). The Elovich parameter α(mg/g/min) and the initial sorption rate β(g/mg),the constant related to the energy of activation extent of surface coverage are evaluated. On analysing the results of Elovich model (Table2),the initial adsorption rate (α) decreases from 0.184 to 0.041 (mg/g/min) and increases from 0.065to 0.085 (g/mg) on increasing the Rh-B concentration and temperature respectively. The increase in concentration reduces the initial sorption rate due to competitive ions, whereas the high temperature favors the initial sorption rate. Another Elovich constant related to the energy of activation and extent of surface coverage (β) increases on increasing the initial Rh-B concentration as well as the system temperature.The r^2 value of Elovich model is comparable with that of

first and second order kinetic model, which indicate the good degree of fitness of the Elovich model to the Rh-B/NCS adsorption system.

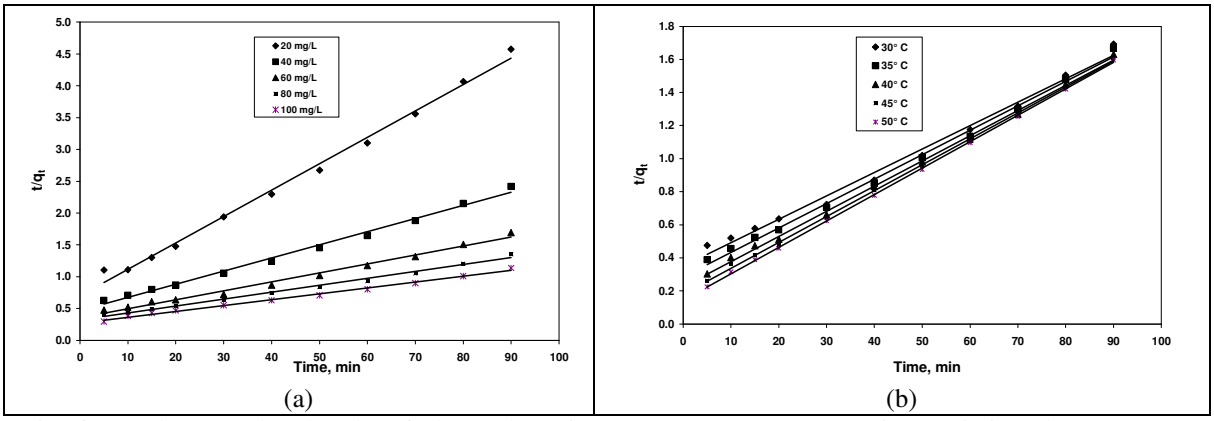

(a) (b)

Fig.-6: Pseudo-Second Order plot of Rh-B Adsorption onto NCS, (a) Concentration Variation, (b) Temperature Variation

Table-2: Kinetic Model Results of Rh-B Adsorption

Parameters	Initial Rh-B Concentration, mg/L					Temperature, °C			
	20	40	60	80	100	35	40	45	50
$q_e$exp.(mg/g)	19.68	37.21	53.14	66.52	79.13	54.00	55.20	55.92	56.33
Pseudo First Order Kinetics									
k_1 x 10^{-2}(min $^{-1}$)	6.425	5.965	5.343	5.758	5.366	5.804	5.527	5.481	5.619
$q_e$cal(mg/g)	21.99	43.35	58.22	84.66	97.23	59.29	53.49	49.29	45.39
r^2	0.9778	0.9669	0.9964	0.9608	0.9622	0.9737	0.9846	0.9896	0.9922
Pseudo Second Order Kinetics									
k_2 x 10^{-3} (g/mg/min)	2.44	0.92	0.56	0.37	0.31	1.035	1.259	1.468	1.773
h	1.4229	2.1409	2.8003	3.1260	3.6900	3.4990	4.4623	5.5249	6.9252
$q_e$cal(mg/g)	24.15	48.31	70.92	91.74	108.70	58.14	59.52	61.35	62.50
r^2	0.994	0.9933	0.9895	0.9929	0.994	0.9958	0.998	0.9991	0.9997
Elovich Model									
α (mg/g/min)	0.184	0.090	0.061	0.048	0.041	0.065	0.070	0.076	0.083
β (g/mg)	2.929	4.415	5.859	6.743	7.955	7.156	9.420	12.662	18.607
r^2	0.9797	0.9849	0.9811	0.9886	0.9836	0.9848	0.981	0.9755	0.9738
Intra Particle Diffusion Model (II step)									
k_{id}(mg/g/min^{½})	3.059	5.993	8.940	10.149	11.595	8.489	8.044	7.618	7.086
r^2	0.9639	0.9935	0.9935	0.9958	0.9986	0.987	0.9705	0.9508	0.956
Intra Particle Diffusion Model (III step)									
k_{id}(mg/g/min^{½})	1.368	3.002	3.579	7.663	8.046	4.146	3.940	3.442	2.310
r^2	0.9743	0.9999	0.9901	0.9985	0.9841	0.9968	0.9999	0.9927	0.9848

Intraparticle Diffusion Model

The intraparticle diffusion plot for Rh-B adsorption into NCS is shown in Fig.-7 and the results are given in Table-2. The plot shows multi linearity with the three different phases.This multi linearity in the plot indicates that there are more than one kinetic stage occurs in the Rh-B/NCS adsorption system[27]. The first linear and fastest process is correlated to the diffusion of Rh-B from the bulk of the solution towards the sorbent surface. The second portion is the intra-particle diffusion of dye molecules, which has moderate velocity and the third phase is the diffusion of Rh-B into the pores of NCS. After the third process, the adsorption attains an equilibrium stage[27]. The intra-particle diffusion rate constant k_{id} was evaluated for the second and third step and reported in the Table-2. (as the first step is the fastest and it is not considered).

The intra-particle diffusion plot indicated that the plot does not pass through the origin, hence it is assumed that intra-particle diffusion is not the sole rate-limiting step. The final stages are predominantly controlled by Intraparticle diffusion and initial stage it may be external mass transfer mechanism[30].

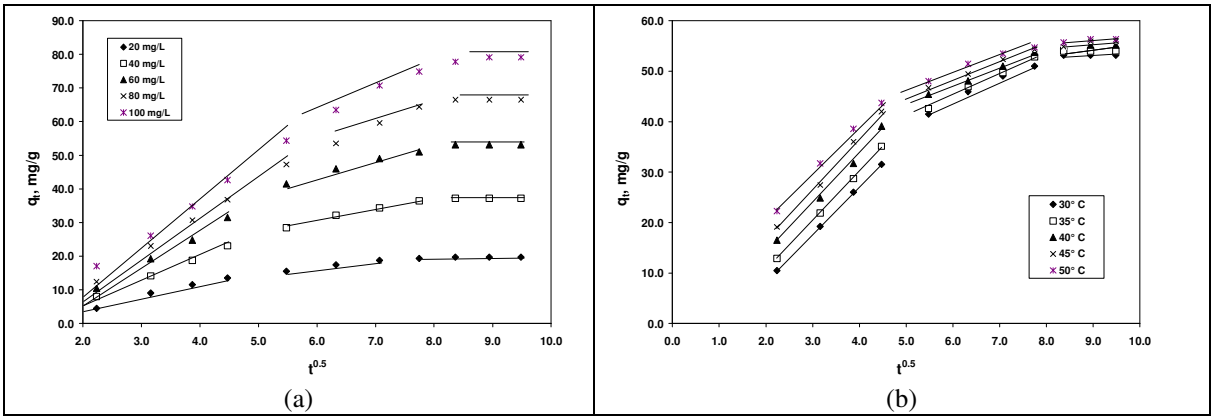

(a) (b)

Fig.-7: Intra-particle Diffusion plot of Rh-B adsorption onto NCS, (a) Concentration Variation, (b) Temperature Variation

Adsorption Isotherm Analysis

The rate of change of adsorbed solute concentration with respect to the concentration of solute in the solution at a given temperature is called as adsorption isotherm. The results of adsorption isotherm give some insights into the nature of the surface, the interaction of the solute with the surface and adsorption mechanisms[31]. In this study, the adsorption data of Rh-B adsorption onto NCS was evaluated using Langmuir (1918) and Freundlich (1906) isotherm models[24]. The isotherm studies were performed at 30,35,40 and 45° C.

The Langmuir plot for Rh-B adsorption onto NCS is given in fig 8a and the results calculated from the slope and intercepts are presented in Table-3. The Langmuir monolayer capacity increases from 78.13 to 80.65 mg/g on increasing the system temperature from 30 to 45° C, which is comparable with the results reported by the previous researchers. Langmuir monolayer capacity (Q_0 mg/g) in the present study is comparable with the past results. The dimensionless equilibrium parameter R_L ranged between 0 to 1.0indicates the favourability of adsorption under the given set of operating conditions.

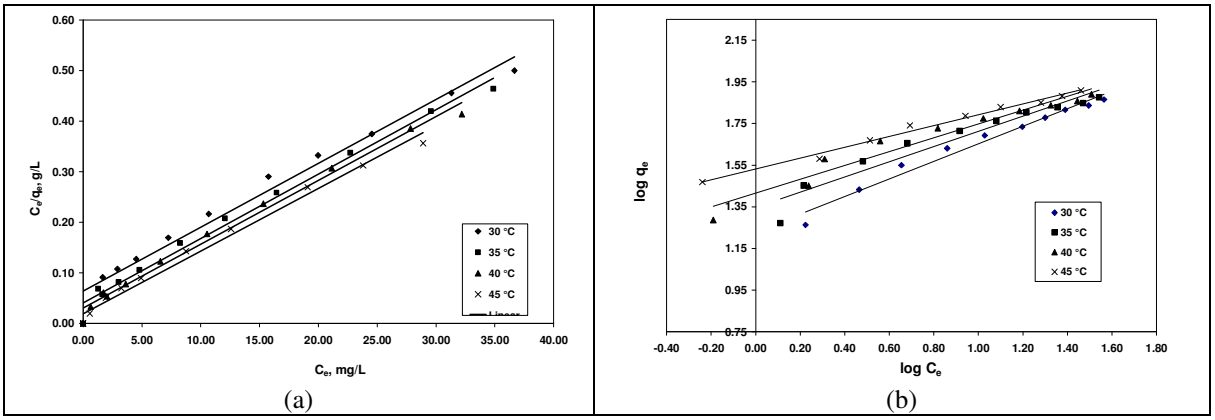

(a) (b)

Fig.-8: Isotherm plot of Rh-B Adsorption onto NCS, (a) Langmuir, (b) Freundlich

The Freundlich adsorption isotherm plot for the adsorption of Rh-B onto NCS is shown in Fig.-8b. The Freundlich isotherm equation is an empirical equation derived with an assumption of the sorption that involves heterogeneous system. There is a logarithmic decrease in the enthalpy of adsorption with an increase in the fraction of occupied sites if the adsorption obeys the Freundlich adsorption model.

The Freundlich constant k_f related to the quantity of dye adsorption for unit equilibrium concentration increased from 17.04 to 34.01 ($mg^{1-1/n}$ $L^{1/n}$ g^{-1}) on increasing the solution temperature from 30 to 45°C.

Another constant 1/n related to the adsorption intensity of dye onto the adsorption intensity of dye onto the adsorbent or surface heterogeneity. If the value of 1/n is closer to zero (the value of n between 1 to 10), the adsorption becomes more and more heterogeneous. As observed from the Table-3, the constant n varied between 2.38 to 3.84, indicating the normal Langmuir type of adsorption involving more surface heterogeneity.

Table-3: Results of Isotherm plots for the Adsorption of Rh-B onto NCS

Parameters	Temperature °C			
	30	35	40	45
Langmuir isotherm				
Q_0 (mg/g)	78.13	78.74	79.37	80.65
b_L x10^{-3}(L/mg)	0.2000	0.3113	0.4145	0.6425
r^2	0.9749	0.9885	0.99	0.9877
Freundlich Isotherm				
n	2.38	2.74	3.02	3.84
k_f ($mg^{1-1/n}$ $L^{1/n}$ g^{-1})	17.04	22.22	26.06	34.01
r^2	0.9729	0.9303	0.9466	0.9884

Thermodynamics of Adsorption

The thermodynamic parameters related to the adsorption are derived from the Van'tHoff plot as shown in fig 9 and the results are shown in table 4. The negative Gibbs free energy change for the adsorption of Rh-B into NCS indicates the favourability of adsorption. As the value of ΔG is more negative at higher temperature indicate that the adsorption of Rh-B is favored by high temperature.

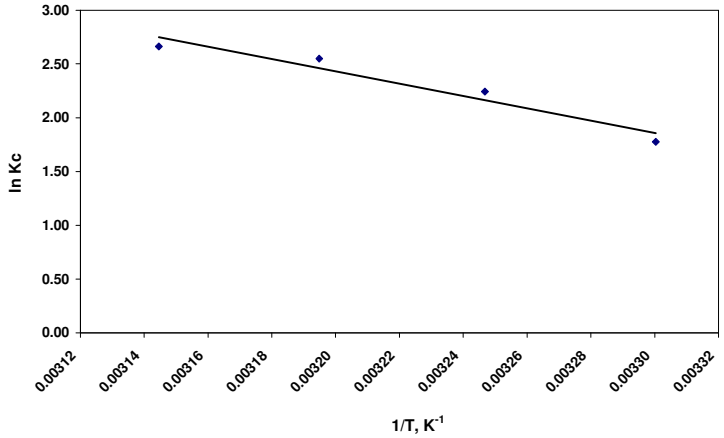

Fig.-9: TD plot of Rh-B Adsorption onto NCS

The enthalpy change for the adsorption is positive; indicate that the adsorption of Rh-B into the NCS surface absorbs energy. The endothermic nature substantiates the chemisorption type of adsorption for Rh-B into NCS surface. Another thermodynamic parameter ΔS,the entropy change decreases on increasing the temperature. At higher temperature, the extent of Rh-B adsorption is more, hence the randomness decreases.

Table-4: Thermodynamic Results of Rh-B Adsorption NCS

Temperature, °C	ΔG, kJ/mol	ΔH, kJ/mol	ΔS, J/K/mol
30	- 4.471	47.757	173.04
35	- 5.742		
40	- 6.634		
45	- 7.039		

CONCLUSION

The study demonstrates that NCS is an effective adsorbent for the removal of Rh-B from its aqueous solution. The adsorbent NCS is capable of removing Rh-B at the maximum of 79.13 mg/g at an initial

Rh-B concentration of 100mg/L. The adsorption is strongly dependent on solution pH and the kinetic studies proved that the adsorption follows pseudo-first order at the initial stages and second order during the later stages of adsorption. The maximum Langmuir monolayer capacity is 80.65 mg/g, which is comparable with other adsorbents reported in the past. The thermodynamic studies indicate the spontaneous, endothermic and decreased randomness of Rh-B adsorption.

REFERENCES

1. L. da Silva Leite, B. de Souza Maselli, G. de AragaoUmbuzeiro and R.F. PupoNogueira, *Chemosphere*, **148**, 511 (2016), **DOI:** 10.1016/j.chemosphere.2016.01.053.
2. H. Altaher, T.E. Khalil and R. Abubeah, *Color Technol*., **130**, 205 (2014), **DOI:** 10.1111/cote.12086.
3. Y.H. Magdy and H. Altaher, *J. Environ. Chem. Eng*., **6**, 834 (2018), **DOI:**10.1016/j.jece.2018.01.009.
4. N.H. Hsu, S.L. Wang, Y.H. Liao, S.T. Huang, Y.M. Tzou and Y.M. Huang, *J. Hazard. Mater*.,**171**, 1066 (2009), **DOI:** 10.1016/j.jhazmat.2009.06.112.
5. S.B. Jadhav and R.S. Singhal, *Int. Biodeterior. Biodegrad*., **85**, 271(2013), **DOI:** 10.1016/j.ibiod.2013.08.009.
6. M. Dastkhoon, M. Ghaedi, A. Asfaram, A. Goudarzi, S.M. Mohammadi and S. Wang, *Ultrason. Sonochem*.,**37**, 94 (2017), **DOI:** 10.1016/j.ultsonch.2016.11.025.
7. G. Moussavi and R. Khosravi, *Chem. Eng. Res. Des*., **89**, 2182 (2011), **DOI:** 10.1016/j.cherd.2010.11.024.
8. W.R.P. Barros, J.R. Steter, M.R.V. Lanza and A.J. Motheo, *Electrochim. Acta*.,**143**, 180 (2014), **DOI:** 10.1016/j.electacta.2014.07.141.
9. N.A. Dahlan and S.L. Ng, J. Pushpamalar, *J. Appl. Polym. Sci*., **134** (2017), **DOI**: 10.1002/app.44271.
10. A.P. Abbott, O. Alaysuy, A.P.M. Antunes and A.C. Douglas, *J. ACS Sustain. Chem. Eng*., **3**, 1241 (2015), **DOI:** 10.1021/acssuschemeng.5b00226.
11. G. Huang, W. Wang and G. Liu, *J. Environ. Manage*.,**157**, 297 (2015), **DOI:** 10.1016/j.jenvman.2015.04.031.
12. R.R. Krishni, K.Y. Foo and B.H. Hameed, *Desalin. Water Treat*.,**52**, 6096 (2014).
13. M.T. Yagub, T.K. Sen, S. Afroze and H.M. Ang, *Adv. Colloid Interface Sci*.,**209**, 172 (2014), **DOI:**10.1016/j.cis.2014.04.002.
14. F.I. Vacchi, P.C. Von der Ohe, A.F. de Albuquerque, J.A.S. de Vendemiatti, C.C.J. Azevedo, J.G. Honório, B.F. da Silva, M.V.B. Zanoni, T.B. Henry, A.J. Nogueira and G.A. de Umbuzeiro, *Chemosphere*, **156**, 95 (2016).
15. K. Ravindhranath and M. Ramamoorty, *Rasayan J. Chem*., **10(3)**, 716 (2017), **DOI:** 10.7324/RJC.2017.1031762
16. S. Deng, Q. Zhou, G. Yu, J. Huang and Q. Fan, *Water Res*., **45**, 1774 (2011), **DOI:** 10.1016/j.watres.2010.11.029.
17. H. L. Yadav and A.Jamal, *Rasayan J. Chem*., **10(3)**, 1062 (2017), **DOI:**10.7324/RJC.2017.1031775.
18. I. Fatimah, B.N. Huda, I.L. Yusuf and B. Hartono, *Rasayan J. Chem*, **11 (3)**, 1166 (2018), **DOI:**10.31788/RJC.2018.1134021.
19. H. JogaRao, P. King and Y. Prasanna Kumar, *Rasayan J. Chem*, **11(3)**, 1376 (2018), **DOI:** 10.31788/RJC.2018.1134035.
20. S. Singh, V.C. Srivastava and I.D. Mall, *J. Phys. Chem. C*, **117**, 15229 (2013), **DOI:** 10.1021/ie4042005.
21. A. Ahmad, S.H. Mohd-Setapar, C.S. Chuong, A. Khatoon, W.A. Wani, R. Kumar and M. Rafatullah, *RSC Adv*.,**5**, 30801 (2015), **DOI:**10.1039/C4RA16959J.
22. R. Drissi and C. Mouats, *Rasayan J. Chem*, **11(3)**, 1126 (2018), **DOI:**10.31788/RJC.2018.1132081.
23. B. Murugesan, A. Sivakumar, A. Loganathan and P. Sivakumar, *J. Taiwan Inst. Chem. Eng*., **71**, 364 (2017), **DOI:**10.1016/j.jtice.2016.11.020.
24. P. Sivakumar and P.**N.**Palanisamy, *Rasayan J. Chem*., **1(4)**, 871 (2008)
25. L.D.T. Prola, E. Acayanka, E.C. Lima, C.S. Umpierres, J.C.P. Vaghetti, W.O. Santos, S. Laminsi and P. Djifon, *Ind. Crop Prod*., **46**, 328 (2013).

26. T. Calvete, E.C. Lima, N.F. Cardoso, S.L.P. Dias and F.A. Pavan, *Chem. Eng. J*., **155**, 627 (2009), **DOI:** 10.1016/j.cej.2009.08.019.
27. W.S. Alencar, E.C. Lima, B. Royer, B.D. dos Santos, T. Calvete, E.A. da Silva and C.N. Alves, *Sep. Sci. Technol*.,**47**, 513 (2012), **DOI:**10.1080/01496395.2011.616568.
28. I.A.W. Tan, A.L. Ahmad and B.H. Hameed, *J. Hazard. Mater*., **164**, 473 (2009), **DOI:**10.1016/j.jhazmat.2008.08.025.
29. S.Saminathan, M. Asaithambi, V. Sivakumar and P. Sivakumar, *Rasayan J. Chem*., **9(4)**, 812 (2016).
30. V. Fierro, V. Torné-Fernández, D. Montané and A. Celzard, *MicroporousMesoporous Mat*., **111**, 276 (2008), **DOI:** 10.1016/j.micromeso.2007.08.002.
31. L.D.T. Prola, F.M. Machado, C.P. Bergmann, F.E. de Souza, C.R. Gally, E.C. Lima, M.A. Adebayo, S.L.P. Dias and T. Calvete, *J. Environ. Manage*., **130**, 166 (2013), **DOI:** 10.1016/j.jenvman.2013.09.003.

[RJC-5027/2018]